

# Mean-field universality class induced by weak hyperbolic curvatures

Andrej Gendiar<sup>1</sup>, Michal Daniška<sup>1</sup>, Roman Krčmár<sup>1,2</sup>, Tomotoshi Nishino<sup>2</sup>

<sup>1</sup>*Institute of Physics, Slovak Academy of Sciences, SK-845 11, Bratislava, Slovakia*

<sup>2</sup>*Department of Physics, Graduate School of Science, Kobe University, Kobe 657-8501, Japan*

(Dated: July 4, 2021)

Order-disorder phase transition of the ferromagnetic Ising model is investigated on a series of two-dimensional lattices that have negative Gaussian curvatures. Exceptional lattice sites of coordination number seven are distributed on the triangular lattice, where the typical distance between the nearest exceptional sites is proportional to an integer parameter  $n$ . Thus, the corresponding curvature is asymptotically proportional to  $-n^{-2}$ . Spontaneous magnetization and specific heat are calculated by means of the corner transfer matrix renormalization group method. For all the finite  $n$  cases, we observe the mean-field-like phase transition. It is confirmed that the entanglement entropy at the transition temperature is linear in  $(c/6) \ln n$ , where  $c = 1/2$  is the central charge of the Ising model. The fact agrees with the presence of the typical length scale  $n$  being proportional to the curvature radius.

PACS numbers: 05.50.+q, 05.70.Jk, 64.60.F-, 75.10.Hk

## I. INTRODUCTION

Quantum and statistical phenomena under non-Euclidean geometry have been attracting research interests in a number of physical systems. For example, experiments on magnetic nano-structures [1–3] have been performed in connection with soft materials exhibiting a conical geometry [4]. One can list investigations on the quantum gravity [5, 6], lattice dislocations of the solid-state crystals, complex networks [7, 8] such as neural systems and complicated web connections.

The focus of the present analysis lies in classical lattice spin models, for which the thermal property is influenced by the non-flatness of the underlying lattice. As typical examples, phase transitions on regular two-dimensional hyperbolic lattices have been studied for the Ising model [9–11], the  $q$ -state clock models [12, 13], the XY-model [14], and the frustrated  $J_1$ - $J_2$  Ising model [15]. In these studies, the hyperbolic lattices are constructed by means of the tessellation of regular polygons with  $p$  sides, where the coordination number,  $q$ , satisfies the hyperbolic condition  $(p-2)(q-2) > 4$ . Such uniform hyperbolic lattices are conventionally called the  $(p, q)$  lattice, and their Hausdorff dimension is infinite [16, 17]. The observed phase transitions in numerical studies qualitatively agree with the mean-field approximation. In particular, the second-order phase transition with the Landau mean-field universality has been observed for the Ising model [18]. The origin of the mean-field behavior has not been clarified yet.

A key feature of the phase transitions on the hyperbolic  $(p, q)$  lattices is that the correlation length remains finite even at the transition temperature [17, 19]. The fact suggests the presence of an inherent length in each  $(p, q)$  lattice, the length which violates the realization of the scale invariance at criticality. One can conjecture that the length is related to the curvature radius  $r = 1/\sqrt{-K}$ , where  $K$  is the Gaussian curvature on a hyperbolic plane. As long as we observe  $(p, q)$  lattices only, it is non-trivial

to confirm this conjecture, since the radius  $r$  is of the order of the lattice constant even on the  $(3, 7)$  lattice, which is less curved than the cases with  $p = 3$  and  $q \geq 8$ .

In this article we propose a way to construct a series of two-dimensional lattices formed by tessellation of the triangles ( $p = 3$ ), where the absolute value of the *averaged* curvature  $K$  is smaller than the  $(3, 7)$  lattice. Such a slightly curved lattice is obtained by distributing exceptional lattice sites of the coordination number seven within the triangular lattice in such manner that the typical distance between nearest exceptional sites is proportional to an integer parameter  $n$ . Under such construction, the corresponding curvature  $K$  is asymptotically proportional to  $n^{-2}$ , and the radius  $r$  is proportional to  $n$ . We calculate thermodynamic properties of the Ising model on the series of weakly curved lattices by means of the corner transfer matrix renormalization group (CTMRG) method [20], which is based on Baxter's corner transfer matrix (CTM) scheme [21]. As a quantity that captures the length scale, we focus on the entanglement entropy at the transition temperature. As we show in the following, the entropy scales as  $(c/6) \ln n$ , where  $c = 1/2$  is the central charge of the Ising model. The fact supports the conjecture on the presence of a finite length scale, which is related to the curvature radius at the transition temperature.

The paper is organized as follows. Section II is devoted to the construction of the series of slightly curved lattices constructed by the triangular tessellation. We evaluate the curvature  $K$  and the corresponding radius  $r$  in two ways, one is the averaged curvature on the whole lattice, and the other one is obtained around the center of the lattice. Both evaluations are in agreement with the asymptotic form of the curvature, which is proportional to  $n^{-2}$ . In Sec. III we derive thermodynamic quantities by means of the CTMRG method, which is modified for the series of the lattices. We obtain the spontaneous magnetization, specific heat, and the entanglement entropy. The obtained results are summarized in the last section.

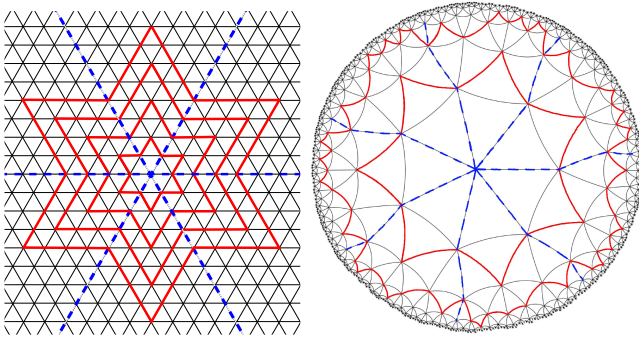


FIG. 1: (Color online) The flat (3,6) lattice on the left and hyperbolic (3,7) one on the right. The blue dashed lines divide each lattice into identical areas, the corners, meeting at the center. The star-shaped area depicted by the thick curves in red show the finite areas of the lattices after  $M$  steps of iterative extensions in Eq. (6).

## II. HYPERBOLIC LATTICES

Throughout this article we consider the Ising model on two-dimensional lattices being either flat or negatively curved. The Hamiltonian is written as

$$H\{\sigma\} = -J \sum_{\langle i,j \rangle} \sigma_i \sigma_j - h \sum_i \sigma_i, \quad (1)$$

where  $\sigma_i = \pm 1$  represents the Ising spin on the lattice site labeled by  $i$ , and the notation  $\langle i,j \rangle$  denotes the nearest neighboring sites. We assume that the interaction is ferromagnetic ( $J > 0$ ) and a constant magnetic field  $h$  is acting equally on each spin site. We always keep in mind the possibility of obtaining the partition function

$$Z = \sum_{\{\sigma\}} \exp \left[ -\frac{1}{k_B T} H\{\sigma\} \right] \quad (2)$$

numerically, by means of the CTMRG method [17, 20]. Under these requirements, we have chosen the following candidates of the curved lattices.

Let us start from the  $(p, q)$  lattice, which is a tessellation of regular polygons with  $p$  sides, where the coordination number around each site is  $q$ . We restrict ourselves to the case of  $p = 3$  throughout this article. Figure 1 shows two examples, a triangular (planar) (3,6) lattice and a hyperbolic (3,7) lattice. The latter is drawn inside the so-called Poincare disk because the (3,7) lattice has a non-Euclidean geometry. Although the triangles inside the Poincare disk are deformed and shrunk toward the border of the circle, which corresponds to the infinity, the interaction coupling  $J$  remains constant everywhere, and so does the actual sizes of the triangles. The blue dashed lines divide the lattice into  $q$  equivalent parts,  $\mathcal{C}$ , which are called the corners.

The (3,  $q$ ) lattice can be constructed by means of recursive extensions [17]. In order to simplify the discussion, we start from the (3,6) lattice. The smallest unit we

consider is not a equilateral triangle. Instead, we chose a rhombus  $\mathcal{W}$  consisting of two adjacent equilateral triangles. We introduce other two objects, parallelograms (or stripes)  $\mathcal{L}_M$  and  $\mathcal{R}_M$  created by joining  $M$  number of rhombi  $\mathcal{W}$  in one direction. Let us write such joining process by using formal recursive equations

$$\begin{aligned} \mathcal{L}_{M+1} &= \mathcal{W} \mathcal{L}_M, \\ \mathcal{R}_{M+1} &= \mathcal{W} \mathcal{R}_M, \end{aligned} \quad (3)$$

initiated from  $\mathcal{L}_1 = \mathcal{R}_1 = \mathcal{W}$ . These products on the right-hand side represent the joining of parts in a pictorial (or diagrammatic) manner. We also need to introduce another extended rhombus  $\mathcal{C}_M$  of the size  $M$  by  $M$  satisfying the formal joining relation

$$\mathcal{C}_{M+1} = \mathcal{W} \mathcal{L}_M \mathcal{C}_M \mathcal{R}_M \quad (4)$$

starting from  $\mathcal{C}_1 = \mathcal{W}$ . We often call  $\mathcal{C}_M$  a corner. Hence, we can consider a star-shaped area proportional to the size  $M$  that is constructed by joining six corners that are formally represented as  $(\mathcal{C}_M)^6$ . The red lines in Fig. 1 (left) bound the areas for the cases  $1 \leq M \leq 4$ . Repeating this extension processes, the star-shaped area of an arbitrary size can be obtained on the (3,6) lattice. The total number of the lattice sites in  $(\mathcal{C}_M)^6$  is  $6(M+1)M+1$ .

A slight modification of the extension processes in Eqs. (3) and (4) enables us to construct the hyperbolic (3,7) lattice, shown in the right side of Fig. 1. In this case, the extensions are formally written as

$$\begin{aligned} \mathcal{L}_{M+1} &= \mathcal{W} \mathcal{L}_M \mathcal{C}_M, \\ \mathcal{R}_{M+1} &= \mathcal{W} \mathcal{C}_M \mathcal{R}_M, \\ \mathcal{C}_{M+1} &= \mathcal{W} \mathcal{L}_M (\mathcal{C}_M)^2 \mathcal{R}_M, \end{aligned} \quad (5)$$

where the details can be found in Ref. [17]. Notice that the extension to the hyperbolic (3,7) lattice also follows a recursive construction. Compared with the extension process in Eqs. (3) and (4) of the (3,6) lattice, the right-hand sides of Eq. (5) contain an extra corner  $\mathcal{C}_M$ , and this insertion realizes the coordination number seven within the whole lattice. The areas on the right side of Fig. 1, bordered by the red lines, correspond to the ‘star-shaped’ lattices  $(\mathcal{C}_1)^7$  and  $(\mathcal{C}_2)^7$ . On the (3,7) lattice, the total number of the lattice sites grows exponentially with  $M$  [22].

Among the (3,  $q$ ) lattices satisfying the hyperbolic condition  $q > 6$ , the (3,7) lattice exhibits the least curvature in the sense that the absolute value of its curvature,  $|K|$ , is the smallest. The curvature radius  $r = 1/\sqrt{-K} \approx 0.917$  is already of the order of the lattice constant [17], in contrast to  $r = \infty$  in the (3,6) lattice. In this respect, the (3,7) lattice is ‘too far’ from the (3,6) lattice. We have to construct such lattices that have the curvature radii in between, i.e.,  $0.917 < r < \infty$ , in order to quantify the effect of the non-zero curvature to the order-disorder phase transition. We, therefore, consider such a lattice that consists of triangles, and the lattice

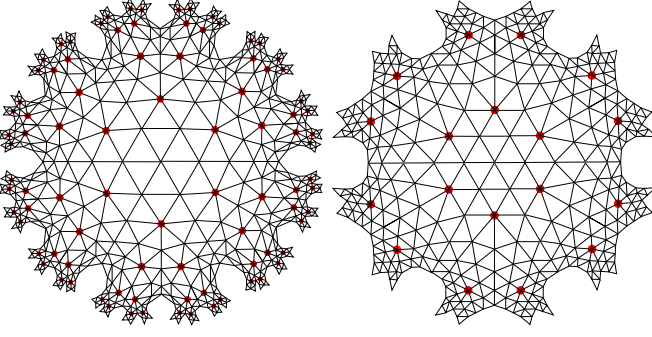


FIG. 2: (Color online) The two typical lattice geometries for  $n = 1$  (left) and  $n = 2$  (right) for the size  $M = 5$ . The filled circles denote the exceptional lattice sites with the coordination number seven, and number of the exceptional sites is 90 in the left and 18 in the right, c.f. Eq.(9).

sites contain a mixture of the coordination numbers six and seven. As the number of the lattice sites with the coordination number seven decreases, such a mixed lattice approaches the flat triangular (3,6) lattice. We use the term ‘exceptional’ lattice site for such sites that have the coordination number seven.

There are many sequential methods to generate mixed lattices. We have chosen the following extension scheme

$$\begin{aligned} \mathcal{L}_{M+1} &= \mathcal{W} \mathcal{L}_M, \\ \mathcal{R}_{M+1} &= \mathcal{W} \mathcal{R}_M, \\ \mathcal{C}_{M+1} &= \begin{cases} \mathcal{W} \mathcal{L}_M (\mathcal{C}_M)^2 \mathcal{R}_M & (\text{at every } n^{\text{th}} \text{ step}), \\ \mathcal{W} \mathcal{L}_M \mathcal{C}_M \mathcal{R}_M & (\text{otherwise}) \end{cases} \end{aligned} \quad (6)$$

to analyze the property of the Ising model on this lattice. These processes are almost the same as the extension scheme in Eqs. (3) and (4) for the (3,6) lattice, but when  $M$  is a multiple of an integer parameter  $n$ , we insert an additional corner  $\mathcal{C}_M$  in the extension process from  $\mathcal{C}_M$  to  $\mathcal{C}_{M+1}$ . This process adds the exceptional lattice site with the coordination number seven whenever  $(M \bmod n) = 0$ . Note that we used the extension process of  $\mathcal{L}_M$  and  $\mathcal{R}_M$  as in Eq. (3). This restriction keeps the corner  $\mathcal{C}_M$  symmetric to the spatial inversion, the property which is convenient for numerical calculations by the CTMRG method. On the other hand, this simplification introduces a slight inhomogeneity to the lattice, which should be considered carefully.

Whenever we obtain the extended corner  $\mathcal{C}_{M+1}$  shown as Eq. (6), we consider the joined lattice area made of the six corners which can be formally represented as  $(\mathcal{C}_{M+1})^6$ . Figure 2 shows the two examples of such ‘star-shaped’ regions for  $M = 5$  in the cases when  $n = 1$  (left) and  $n = 2$  (right). The filled dots (in red) emphasize those exceptional lattice sites, where the additional corners have been inserted.

### A. Coordination number

Looking at the extension process in Eq. (6), one finds that total number of the lattice sites  $\mathcal{N}_n(M)$  exponentially increases with  $M$  for arbitrary finite  $n$ . When  $n$  is a multiple of  $M$ , this counting is easily performed by a recursive formula shown in Appendix, and generalization to the arbitrary  $n$  is straightforward. Having counted the total number of the lattice sites in the whole lattice area  $(\mathcal{C}_M)^6$  created by Eq. (6), we obtain

$$\mathcal{N}_n(M) = 1 + 12 \sum_{j=1}^M j 2^{k_n(nk_n(M,1)+n,j)}, \quad (7)$$

where we introduced a double-nested greatest integer (floor) function in the exponent; the floor function has the following form

$$k_n(m, j) = \left\lfloor \frac{m-j}{n} \right\rfloor \equiv \max \left\{ i \in \mathbb{Z} \mid i \leq \frac{m-j}{n} \right\}. \quad (8)$$

In the same manner, we can obtain the number of the exceptional sites

$$\mathcal{S}_n(M) = 6 \left[ 2^{k_n(M,1)} - 1 \right] \quad (9)$$

for any set of  $n$  and  $M$ . This number is consistent with the cases shown in Fig. 2, where  $\mathcal{S}_1(5) = 90$  on the left and  $\mathcal{S}_2(5) = 18$  on the right.

Considering the asymptotic limit  $M \rightarrow \infty$ , the ratio between  $\mathcal{S}_n(M)$  and  $\mathcal{N}_n(M)$  leads to the average density of the exceptional sites

$$\lim_{M \rightarrow \infty} \frac{\mathcal{S}_n(M)}{\mathcal{N}_n(M)} = \frac{1}{2n(3n+1)}. \quad (10)$$

For sufficiently large  $n$ , the density becomes proportional to  $n^{-2}$ . For the brevity, we introduce the averaged coordination number

$$q_n = 6 + \frac{1}{2n(3n+1)}. \quad (11)$$

Note that  $q_\infty = 6$  is the coordination number of the (3,6) lattice [23]. Using the notation  $q_n$  thus defined, we denote the lattice constructed by Eq. (6) as the (3,  $q_n$ ) lattice.

Length of the system lattice border,  $\mathcal{P}_n(M)$ , is another essential quantity that characterizes the geometry of the (3,  $q_n$ ) lattice. The analytic formula of  $\mathcal{P}_n(M)$  can be obtained as

$$\mathcal{P}_n(M) = 12 \left[ M - nk_n(M,1) + n \sum_{j=1}^{k_n(M,1)} 2^j \right], \quad (12)$$

where a simple derivation is presented in the Appendix. It should be noted that the ratio of the boundary sites

to the total number of the lattice sites in the asymptotic limit

$$\lim_{M \rightarrow \infty} \frac{\mathcal{P}_n(M)}{\mathcal{N}_n(M)} = \frac{2}{3n+1} \quad (13)$$

is finite and inversely proportional to  $n^{-1}$ . Such a dominance of the boundary sites over all lattice sites is a characteristic feature of hyperbolic lattices. Our research target, the thermodynamic property of the system at the center of the  $(3, q_n)$  lattice, is thus surrounded by a wide system boundary which increases exponentially.

### B. Averaged curvature

Now, let us focus our attention to the curvature of the  $(3, q_n)$  lattice. If one looks at a small region that does not contain any exceptional lattice sites, the region is identical to the  $(3, 6)$  lattice as long as the connection of the lattice sites is concerned. The hyperbolic nature of the  $(3, q_n)$  lattice arises from the presence of the exceptional lattice sites which are distributed in a sparse manner. Thus, when we consider the curvature of the  $(3, q_n)$  lattice, we have to take a certain average over the system. Apparently such an averaged curvature is dependent to the parameter  $n$ , and we write it as  $K_n$  in the following. Roughly speaking,  $K_n$  should be proportional to  $n^{-2}$  since the natural scale of the  $(3, q_n)$  lattice is given by  $n$ . We evaluate the averaged curvature by

$$K_n = -r_n^{-2}, \quad (14)$$

where  $r_n$  is the corresponding curvature radius using a geometrical formula [16]

$$\cosh \frac{1}{2r_n} = \frac{\cos \frac{\pi}{3}}{\sin \frac{\pi}{q_n}} \quad (15)$$

on a hyperbolic triangle that consists the  $(3, q_n)$  lattice. We have chosen the lattice constant as the unit of the length. Substituting the asymptotic expression  $q_n = 6 + 1/6n^2$  from Eq. (11) into Eq. (15), we obtain

$$K_n \sim -\frac{2}{3\pi} n^{-2} \quad (16)$$

with the dominant coefficient  $2/3\pi \approx 0.212$  for large  $n$ .

Complementing the evaluation of the averaged curvature, we relate the length of the lattice boundary,  $\mathcal{P}_n(M)$ , to the curvature radius  $r_n$  on a hyperbolic plane

$$\mathcal{P}_n(M) \propto 2\pi \sinh \frac{M}{r_n}. \quad (17)$$

Using Eq. (14) and taking the limit  $M \rightarrow \infty$ , we obtain

$$K_n \sim -(\ln 2)^2 n^{-2}, \quad (18)$$

where the prefactor  $(\ln 2)^2 \approx 0.48$ . To summarize, we have evaluated the averaged curvature on the  $(3, q_n)$  plane in two ways, and both of them lead to  $K_n \propto -n^{-2}$ .

## III. NUMERICAL RESULTS

In this section we study the phase transition of the Ising model on the sequence of the non-Euclidean  $(3, q_n)$  lattices, in particular,

$$(3, q_1), (3, q_2), (3, q_3), \dots, (3, q_\infty). \quad (19)$$

The Hamiltonian is given by Eq. (1), and without loss of generality, the coupling constant  $J$  and the Boltzmann constant  $k_B$  are chosen to be unity. All thermodynamic functions are considered in dimensionless units. Since the elementary unit of  $(3, q_n)$  lattice is the rhombus-shaped  $\mathcal{W}$ , it is natural to attribute the Boltzmann weight to each  $\mathcal{W}$ . Suppose that the Ising spins  $\sigma_i, \sigma_j, \sigma_k$ , and  $\sigma_l$  are placed on the corners of the rhombus. The corresponding Boltzmann weight  $\mathcal{W}$  is given by

$$\mathcal{W}(\sigma_i \sigma_j \sigma_k \sigma_l) = \exp \left\{ \frac{J}{2k_B T} (\sigma_i \sigma_j + \sigma_j \sigma_k + \sigma_k \sigma_l + \sigma_l \sigma_i + 2\sigma_j \sigma_l) + \frac{h}{6k_B T} (\sigma_i + 2\sigma_j + \xi \sigma_k + 2\sigma_l) \right\}, \quad (20)$$

where the diagonal interaction acts between the spins  $\sigma_j$  and  $\sigma_l$ . The pre-factor  $\xi$  is normally unity, and is set to zero when over-counting of interaction with external field  $h$  happens at each exceptional lattice point. Most of the numerical calculations are performed under  $h = 0$  in the following; the only exception is when we observe the magnetic response at the transition temperature.

Taking the tensor product among weights  $\mathcal{W}$ , one can gradually expand the size of the Boltzmann weights  $\mathcal{L}_M$  and  $\mathcal{R}_M$ . These weights are called the half-row transfer matrices. Analogously, the expanding weight  $\mathcal{C}_M$  is called the corner transfer matrix. The procedure of obtaining the transfer matrices represent a generalized version of the CTMRG method applied to the  $(3, 7)$  lattice which is studied in detail in Ref. [17]. Consequently, the ‘reduced’ density matrix is a partial trace of the corner transfer matrices

$$\rho_n(M) = \text{Tr}' [\mathcal{C}_M]^6, \quad (21)$$

where we explicitly include the parameter  $n$  in  $\rho_n(M)$ . In the following we omit the size dependence on  $M$  of the reduced density matrix to simplify the formulae. Taking the complete trace of the reduced density matrix leads to the partition function [20]

$$Z_n = \text{Tr} \rho_n \quad (22)$$

of the star-shaped lattice area.

In our numerical calculations by CTMRG, we keep up to  $m = 200$  block spin states [9, 18, 20], where we have confirmed that all the data are converged with respect to  $m$ . As the system size  $M$  increases,  $\mathcal{C}_M$  approaches its thermodynamic limit during the numerical calculations. Note that  $\mathcal{C}_M$  possesses a minor dependence on  $M$ , since

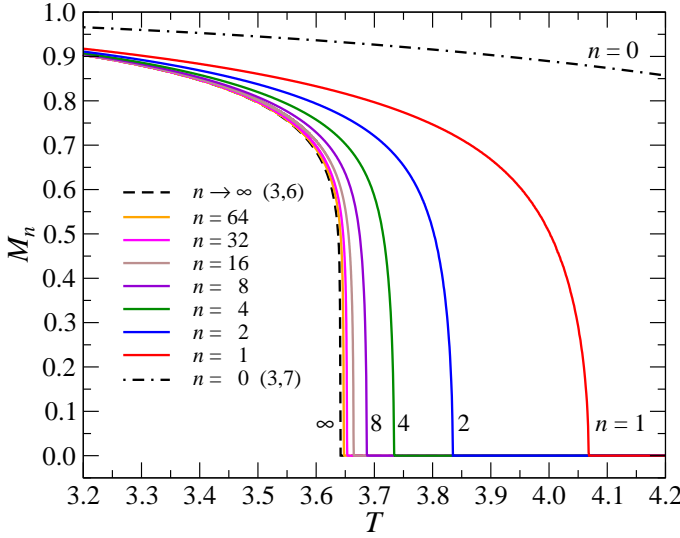


FIG. 3: (Color online) Temperature dependence of the spontaneous magnetization  $M_n(T)$  on the  $(3, q_n)$  and  $(3, 7)$  lattices [17].

we keep inserting of the exceptional lattice sites at every  $n^{\text{th}}$  extension step in accord with Eq. (6). We can either consider the cases where  $M$  is multiple of  $n$  or take the average among the minor fluctuations. There is, however, no qualitative difference in the two choices, and we have chosen the latter one. It should be noted that we focus on the thermodynamic quantity deep inside the system, and discard those phenomena near the system boundary, as we have considered in the previous studies. [17]

Spontaneous magnetization provides information in the ordered phase. Figure 3 displays the temperature dependence of the bulk spontaneous magnetization

$$M_n(T) = \frac{\text{Tr}(\sigma_c \rho_n)}{\text{Tr} \rho_n} \quad (23)$$

at  $h = 0$ , the value which measures the average polarization of the spin  $\sigma_c$  at the center of the lattice system. For comparison, we also show the magnetization on the flat  $(3, 6)$  lattice, denoted by  $n \rightarrow \infty$ , as well as on the hyperbolic  $(3, 7)$  lattice, denoted by  $n = 0$  [17]; we use the analogous notation (by the subscript  $n$ ) for other thermodynamic quantities. The phase transition temperature  $T_n$  monotonously decreases with  $n$  and approaches the analytically known values  $T_\infty = 4/\ln 3 \sim 3.64096$  [21] on the flat  $(3, 6)$  lattice. Roughly speaking, the difference  $T_n - T_\infty$  is inversely proportional to  $n$ .

Just below the transition temperature the power-law behavior

$$M_n(T) \propto (T_n - T)^{\beta_n}, \quad (24)$$

is expected. In order to detect the magnetic exponent  $\beta_n$  from the numerically calculated  $M_n(T)$ , we use the derivative

$$\beta_n(T) = \frac{\partial \ln M_n(T)}{\partial \ln (T_n - T)}, \quad (25)$$

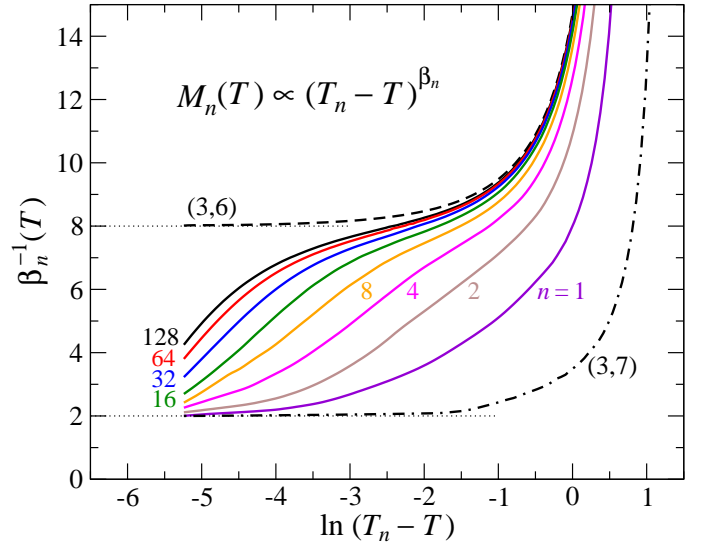


FIG. 4: (Color online) Inverse of the effective magnetic exponent  $\beta_n(T)$  as a function of the logarithmic distance from the transition temperature.

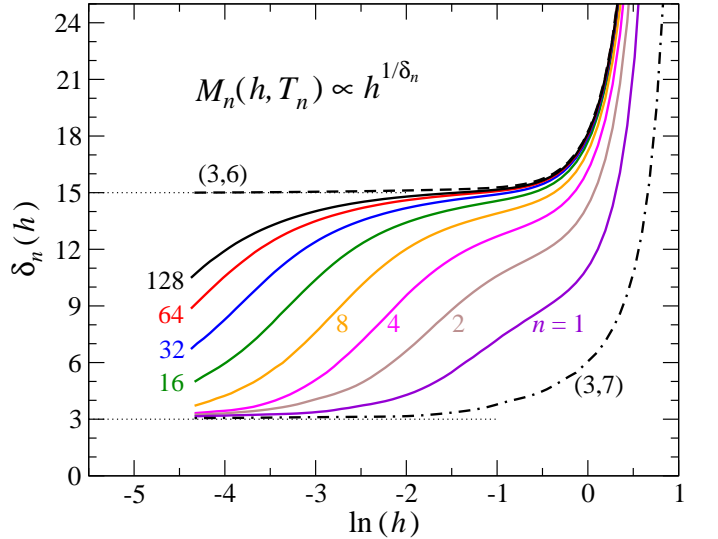


FIG. 5: (Color online) Effective exponent  $\delta_n(h)$  with respect to the logarithm of the external magnetic field at the phase transition temperature  $T_n$ .

within the ferromagnetic ordered phase  $T \leq T_n$ . Figure 4 shows  $\beta_n(T)$  thus obtained. When  $T_n - T$  is relatively large,  $\beta_n(T)$  follows the Ising universality where  $\beta = \frac{1}{8}$ , however, in the neighborhood of the transition temperature  $T_n$ , the magnetic exponent  $\beta_n$  for finite  $n$  increases and tends to  $\beta_n = \frac{1}{2}$ , the value which represents the mean-field universality class.

In addition, we studied the exponent  $\delta$  which is associated with the response of the magnetization to a uniform magnetic field  $h$  at the phase transition temperature  $T_n$ ,

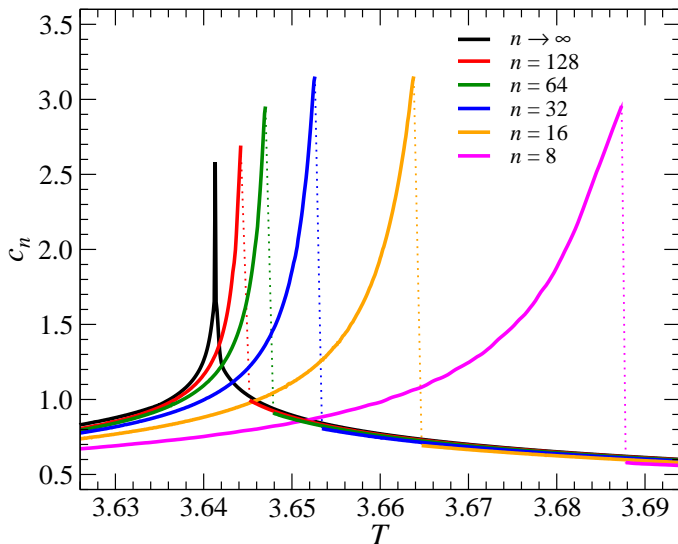


FIG. 6: (Color online) The specific heat on the  $(3, q_n)$  lattice.

which obeys the scaling

$$M_n(h, T_n) \propto h^{1/\delta_n} \quad (26)$$

on the planar lattice. Figure 5 shows the effective critical exponent

$$\delta_n(h) = \left[ \frac{\partial \ln M_n(h, T_n)}{\partial \ln h} \right]^{-1} \quad (27)$$

in the limit  $h \rightarrow 0$ . The observed behavior qualitatively agrees with that of the magnetic exponent  $\beta$  depicted in Fig. 4; the Ising universality  $\delta = 15$  is recovered for the  $(3, 6)$  lattice only. It is obvious that the effective exponent  $\delta_n(h)$  deviates from the Ising one when the external field becomes small, and it again approaches the mean-field value  $\delta_n(h \rightarrow 0) = 3$  for any finite  $n$ .

The internal energy at the center of the system is represented as

$$U_n(T) = -J \frac{\text{Tr}(\sigma_c \sigma_{c'} \rho_n)}{\text{Tr} \rho_n}, \quad (28)$$

where  $\sigma_c$  and  $\sigma_{c'}$  are, respectively, the spin at the center of the system and a neighboring one. Figure 6 shows the specific heat  $c_n(T)$ , which is obtained by taking the numerical derivative of  $U_n(T)$  with respect to the temperature  $T$ . The maxima of the specific heat for large  $n$  are not obtained precisely, because  $U_n(T)$  around  $T = T_n$  is very sensitive to a tiny numerical error. The discontinuity in  $c_n(T)$  for finite  $n$  supports the fact that the transition is of the mean-field nature. Note that small differences of the specific heat,  $c_n(T)$ , in the disordered region  $T \geq T_n$  for various  $n$  is close to  $c_\infty(T)$  on the flat  $(3, 6)$  lattice. This suggests a transient behavior from the Ising universality to the mean-field one which happens within the disordered phase.

As an independent measure of the phase transition, we look at the entanglement entropy  $S_n$ , which can be

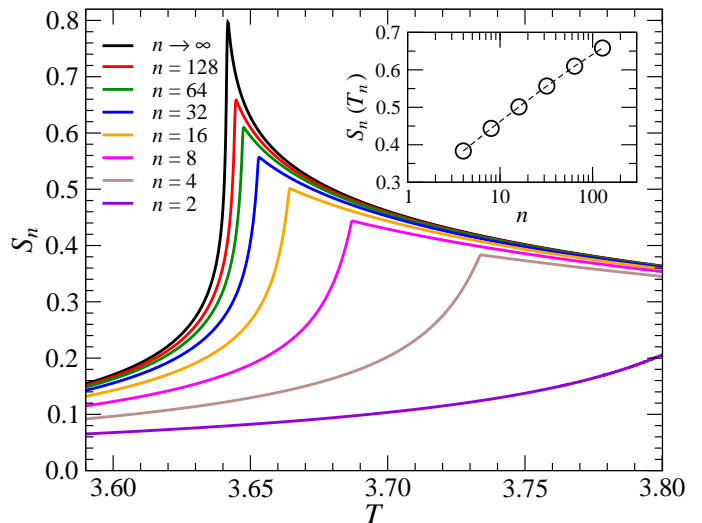


FIG. 7: (Color online) Temperature dependence of the entanglement entropy with respect to  $n$ .

directly computed from the reduced density matrix spectrum

$$S_n(T) = -\text{Tr}(\rho_n \ln \rho_n), \quad (29)$$

where the reduced density matrices are normalized satisfying the condition  $\text{Tr} \rho_n = 1$ . Figure 7 shows  $S_n(T)$ , where the peak values,  $S_n(T_n)$ , are shown in the inset. If the curvature radius  $r_n$  controls the typical length scale at the transition temperature, it is expected that  $S_n(T_n)$  behaves as

$$S_n(T_n) \sim \frac{c}{6} \ln r_n, \quad (30)$$

where  $c$  is the central charge of the system. As shown in Fig. 7, the increase in  $S_n(T_n)$  is close to the value  $(\ln 2)/12 = 0.05776$  when  $n$  doubles, and the fitted value of the slope in the inset gives  $c \sim 0.48$ . This value is consistent with  $c = 1/2$  in the Ising universality class. For this reason, our conjecture about the presence of the typical length scale at  $T_n$ , which is proportional to  $n$  ( $r_n \propto 1/n$ ), is numerically supported.

#### IV. CONCLUSIONS

We have investigated the thermodynamic property of the Ising model on the slightly curved  $(3, q_n)$  lattices, where  $q_n$  represents the averaged coordination number. We used the CTMRG method to calculate the thermodynamic functions deep inside the system around the phase transition temperature. Spontaneous magnetization suggests a transient behavior from the Ising universality class to the mean-field one. The specific heat shows a similar transient behavior from the high temperature side. The entanglement entropy calculated by the density matrix spectra takes its maximum at the phase transition



temperature, where the peak value is proportional to the logarithm of the curvature radius of the  $(3, q_n)$  lattice. These facts support the presence of a finite thermodynamic length scale at the transition temperature which is proportional to the curvature radius. Far away from the transition temperature, the thermal correlation length is much shorter than  $n$ , therefore, there is no difference between the flat  $(3, 6)$  and the  $(3, q_n)$  lattices as long as the thermal property is concerned. As the temperature approaches the transition temperature, the presence of the length scale prevents the realization of the criticality without the typical length scale. This could be the reason of the transient behavior from the Ising universality to the mean-field one.

### Acknowledgments

A. G. thanks Frank Verstraete, Sabine Andergassen, and Vladimír Bužek for inspiring discussions and comments. This work was supported by the European Union projects SIQS, meta-QUTE NFP26240120022, QIMABOS APVV-0808-12, and VEGA-2/0074/12. T. N. and A. G. acknowledge the support of Grant-in-Aid for Scientific Research. R. K. thanks for the support of Japanese Society for the Promotion of Science P12815.

### Appendix A: Number of sites

Let us shortly explain another way to count the number of the lattice sites when the system size  $M$  is a multiple of  $n$ . The extension process in Eq. (6) describes the whole lattice by the extended rhombi of the size  $n$  by  $n$  when the system size  $M$  is the multiple of  $n$ . In such cases, two lattices with different indices  $n$  and  $n'$  are mutually similar, where  $n$  and  $n'$  determine their geometrical scale. We observe a “mixed lattice” under the condition

$$M = nX, \quad (\text{A1})$$

where  $X$  is a positive integer.

Let us count the number of all lattice points in the corner  $\mathcal{C}_M$  when  $M = nX$ . We introduce a notation

$f^{(X)}$  for this number. One finds that there is a recursion relation

$$f^{(X)} = 2f^{(X-1)} - [n(X-1) + 1] + (nX + 1)^2 - [n(X-1) + 1]^2, \quad (\text{A2})$$

where the initial condition is given by

$$f^{(1)} = (n + 1)^2. \quad (\text{A3})$$

Solving the recursion relation, we have

$$f^{(X)} = 2^{X-1}(6n^2 + 2n) - (2n^2 - n)X - 3n^2 - n + 1. \quad (\text{A4})$$

In the same manner, we can obtain the number of the special points  $g^{(X)}$  inside the corner  $\mathcal{C}_{M=nX}$ , where the recursion relation in this case can be written as

$$g^{(X)} = 2g^{(X-1)} + 1 \quad (\text{A5})$$

starting with the initial condition  $g^{(1)} = 0$ . We get

$$g^{(X)} = 2^{X-1} - 1. \quad (\text{A6})$$

To count the length of the lattice border, we introduce the number of the border sites  $h^{(X)}$  on the corner  $\mathcal{C}_{M=nX}$ , where the border length of the star-shaped region  $(\mathcal{C}_{M=nX})^6$  is  $6h^{(X)} - 6$ . The recursion relation,

$$h^{(X)} = 2h^{(X-1)} - 1 + 2(n + 1) - 2 \quad (\text{A7})$$

starting from the initial condition

$$h^{(1)} = 2n + 1, \quad (\text{A8})$$

draws the analytic form of the length

$$h^{(X)} = 2^{X+1}n - 2n + 1. \quad (\text{A9})$$

Expressions for  $\mathcal{N}_n(M)$ ,  $\mathcal{S}_n(M)$ , and  $\mathcal{P}_n(M)$  for arbitrary  $M$  are easily obtained if one considers the fact that these numbers change polynomially with respect to  $M$  between  $M = nX$  and  $M = (n + 1)X$ ; the exponential increase of the lattice sites happens only when the additional corners are inserted in each  $n^{\text{th}}$  step.

- 
- [1] H. Yoshikawa, K. Hayashida, Y. Kozuka, A. Horiguchi, and K. Agawa, Appl. Phys. Lett. **85**, 5287 (2004).
  - [2] F. Liang, L. Guo, Q.P. Zhong, X.G. Wen, C.P. Chen, N.N. Zhang, and W.G. Chu, Appl. Phys. Lett. **89**, 103105 (2006).
  - [3] A. Cabot, A. P. Alivisatos, V. F. Puentes, L. Balcells, O. Iglesias, and A. Labarta, Phys. Rev. B **79**, 094419 (2009).
  - [4] W.A. Moura-Melo, A.R. Pereira, L.A.S. Mol, A.S.T. Pires, Phys. Lett. A **360**, 472 (2007).
  - [5] V.A. Kazakov, Phys. Lett. A **119**, 140 (1986).

- [6] C. Holm and W. Janke, Phys. Lett. B **375**, 69 (1996).
- [7] D. Krioukov, F. Papadopoulos, A. Vahdat, and M. Boguñá, Phys. Rev. E **80**, 035101 (2009).
- [8] D. Krioukov, F. Papadopoulos, M. Kitsak, A. Vahdat, and M. Boguñá, Phys. Rev. E **82**, 036106 (2010).
- [9] K. Ueda, R. Krcmar, A. Gendiar, and T. Nishino, J. Phys. Soc. Japan **76**, 084004 (2007).
- [10] H. Shima and Y. Sakaniwa, J. Phys. A **39**, 4921 (2006).
- [11] Y. Sakaniwa, H. Shima, Phys. Rev. E **80**, 021103 (2009).
- [12] A. Gendiar, R. Krcmar, K. Ueda, and T. Nishino, Phys.

- Rev. E **77**, 041123 (2008).
- [13] S.K. Baek, P. Minnhagen, H. Shima, and B.J. Kim, Phys. Rev. E **80**, 011133 (2009).
  - [14] S.K. Baek, H. Shima, and B. J. Kim, Phys. Rev. E **79**, 060106(R) (2009). Academic Press, London, 1982.
  - [15] R. Krcmar, T. Iharagi, A. Gendiar, and T. Nishino, Phys. Rev. E **78**, 061119 (2008).
  - [16] R. Mosseri and J. F. Sadoc, J. Physique Lett. **43**, 249 (1982).
  - [17] A. Gendiar, R. Krcmar, S. Andergassen, M. Daniška, and T. Nishino, Phys. Rev. E **86**, 021105 (2012).
  - [18] R. Krcmar, A. Gendiar, K. Ueda, and T. Nishino, J. Phys. A **41**, 125001 (2008).
  - [19] T. Iharagi, A. Gendiar, H. Ueda, and T. Nishino, J. Phys. Soc. Jpn. **79**, 104001 (2010).
  - [20] T. Nishino, J. Phys. Soc. Jpn. **65**, 891 (1996).
  - [21] R.J. Baxter, Exactly Solved Models in Statistical Mechanics,
  - [22] Total number of the vertices in the  $(3, 7)$  lattice geometry, say  $1 + 7\Gamma_M$ , is given by calculating the recurrence relation  $\Gamma_M = 4\Gamma_{M-1} - \Gamma_{M-2} + 2$  initialized by  $\Gamma_0 = 0$  and  $\Gamma_1 = 2$ . It results  $\Gamma_M = (\Delta_+^{2M+1} - \Delta_-^{2M+1})/(\sqrt{6}-1)$  for which  $\Delta_{\pm} = \sqrt{2 \pm \sqrt{3}}$ . Hence, the asymptotic behavior of  $1 + 7\Gamma_M$  is proportional to  $(2 + \sqrt{3})^M$ .
  - [23] The total number of the sites on the  $(3, 6)$  lattice is  $\lim_{n \rightarrow \infty} \mathcal{N}_n(M) = 1 + 12 \sum_{j=1}^M j 2^0 = 1 + 6M(M+1)$ .